

Atomic distributions across metal–III-V-compound-semiconductor interfaces

D. M. Hill, F. Xu, Zhangda Lin,* and J. H. Weaver

Department of Chemical Engineering and Materials Science, University of Minnesota, Minneapolis, Minnesota 55455

(Received 23 September 1987)

The distribution of atomic species across metal–III-V-compound-semiconductor interfaces has been studied with Ar^+ -ion bombardment and x-ray photoemission complemented by synchrotron radiation photoemission. Results for (Ti, Cr, Co, Au)/GaAs, (Co, Cr)/InP, and (Cr, Au)/InSb show that room-temperature metal deposition induces substrate disruption. The details of reactions at these interfaces then play a critical role in determining the distribution of semiconductor atoms in the overlayers. Strong metal-anion reactions cause the expulsion of cations from regions where there is compound formation, and there is a characteristic coverage at which this occurs. The result is a cation-deficient region near the buried interface. Weak metal-anion reactions cause no such long-range species redistribution, except for surface segregation. For Au–III-V interfaces, there is an onset for anion surface segregation as a nearly pure Au layer decorated by semiconductor atoms in supersaturation evolves from the Au-anion-cation mixture found at low coverage. The driving force for atomic redistribution is the lowering in energy of the system, but this is restricted by kinetics and diffusion at low temperature. Studies for Cr/GaAs show the effect of altering the temperature and, hence, the amount of diffusion.

INTRODUCTION

The properties of interfaces formed by the vapor deposition of metal adatoms at room temperature onto III-V compound-semiconductor surfaces have been studied extensively. The development of experimental techniques that allow interface investigations with atomic resolution has rapidly advanced the understanding of Schottky barrier formation, chemical reaction, and interdiffusion.^{1–10} At the same time, our understanding of the processes and the mechanisms of the interface formation is still far from complete.

One of the most important problems encountered when modeling metal-semiconductor junctions relates to the distributions of the different species and the mechanisms which control these distributions. In this paper we report a systematic study of atomic distributions for metal–III-V compound-semiconductor interfaces formed at room temperature, with or without subsequent annealing. Our goals are to elucidate the factors which control intermixing and to show how they change as an interface evolves. These investigations have focused on the very reactive Ti/GaAs, Cr/InP, Cr/InP, Cr/InSb, and Co/InP interfaces; the mildly reactive Cr/GaAs interface; the nonreactive but disruptive Au/GaAs and Au/InSb interfaces; and the nonreactive, disruptive epitaxial Co/GaAs interface. We have combined high-resolution x-ray photoemission with Ar^+ ion bombardment to demonstrate that the concentration profiles are determined in large measure by the detailed chemical reactions between the deposited metal adatoms and the released anions. We have used results from high-resolution synchrotron radiation core-level photoemission studies to provide complementary information about the onset of surface segregation.

Substrate disruption has been observed in *all* cases, and

there is frequently surface segregation of one or both of the semiconductor species. When strong metal-anion reaction occurs, there is the expulsion of cations from the region where compounds form. This results in the formation of a cation-deficient region near the interface. In contrast, when the reactions are weak there is only limited intermixing at the interface, but no substantial redistribution of semiconductor atoms. Au overlayers on GaAs and InSb are important exceptions since there is substrate disruption but minimal reaction and there is a critical coverage above which *anion* segregation occurs. These atomic redistributions reflect the tendency of the system to minimize its total energy. They show how minimum energy configurations change as the nominal overlayer thickness varies. They also show the metastability with respect to temperature.

EXPERIMENTAL TECHNIQUES

The sputter depth profile measurements were done with a differentially pumped Leybold-Heraeus Ar^+ sputtering gun and a Surface Science Instruments SSX-100-03 x-ray photoelectron spectrometer. Monochromatic Al $K\alpha$ radiation was used throughout, the x-ray spot diameter was 1000 μm , and the analyzer was operated at a pass energy of 150 eV. Photoelectrons were collected at an emission angle of 60° with respect to the surface normal with a half-angle of acceptance of 15° . The experiments were performed in an ultrahigh vacuum system having a base pressure of 5×10^{-11} Torr. During the sputtering measurements, the chamber pressure rose to 2×10^{-8} Torr and was maintained with a cryopump to prevent Ar loading of the ion pumps. A complete description of the experimental system can be found elsewhere.^{11,12}

Synchrotron radiation photoemission experiments were

done at the Aladdin facility at the Wisconsin Synchrotron Radiation Center. The overall experimental energy resolution was optimized for core-level studies of reacting or disrupting interfaces. Core-level intensities were measured as a function of metal coverage to determine the rate at which each species was attenuated by the overlayer, using procedures described in detail elsewhere.¹³ Exponential attenuation with a $1/e$ length equal to the photoelectron mean free path would indicate layer by layer growth whereas more complex behavior would indicate disruption, reaction, or segregation. In this paper, we include attenuation results only for Co/InP(110), Cr/GaAs(110), and Au/GaAs(110) to provide insight into the morphology of the overlayer and the distribution of atoms across the interface for these representative systems.

GaAs(100) and InSb(111) wafers (Si-doped, n -type at 10^{18} cm^{-3} and Cd-doped, p -type at 10^{14} cm^{-3} , respectively) that were oriented to within 0.5° were cleaned with standard etching procedures before insertion into the vacuum chamber. Ar^+ sputtering and annealing (500°C for 30 min for GaAs, 350°C for 40 min for InSb) produced reconstructed $c(8 \times 2)$ and (2×1) surfaces, respectively. GaAs(110) and InP(110) surfaces (Si-doped, n -type at 10^{18} cm^{-3} and Sn-doped, n -type at $4 \times 10^{17} \text{ cm}^{-3}$, respectively) were obtained by cleaving single crystal bars *in situ* to obtain high-quality, mirrorlike surfaces. The metals Ti, Cr, Co, and Au were evaporated from resistively heated W boats at pressures below 2×10^{-10} Torr. The amount of metal deposited was monitored with Inficon quartz-crystal oscillators adjacent to the samples. The sample-to-source distance was ~ 30 cm and the typical evaporation rate was $1 \text{ \AA}/\text{min}$. For studies conducted at high temperature, the wafers were heated from the back with a W filament. The temperatures were determined with an infrared pyrometer with an absolute accuracy of $\pm 15^\circ\text{C}$ and reproducibility of $\pm 5^\circ\text{C}$.

In these experiments we alternately sputtered with 3.5-keV Ar^+ ions and measured the core-level x-ray photoemission spectra for the metal and semiconductor atoms. The sputter profiles were obtained by determining the integrated core emission of the various elements as a function of sputter time following s -shaped background subtraction. In the results presented here, the integrated areas have been normalized to the data acquisition time and are plotted versus time. Sputtering intervals were typically 1–3 min and x-ray photoemission spectroscopy (XPS) measurement of all of the core levels of interest took 5–7 min.

Sputter profiling is not free of pitfalls related to the destructive character of atom removal and the complex morphologies of interfaces. First, inspection of all of the results summarized in Figs. 1–4 shows that the cation intensities cross over those of the anions after prolonged sputtering and the substrate is reached. This preferential anion sputtering and cation enrichment is a well-known and unavoidable phenomenon for III-V semiconductors.^{14,15} Second, structure in the sputter profiles is broadened by the relatively large mean-free paths of the photoelectrons ($15\text{--}20 \text{ \AA}$) and, therefore, the limited depth resolution of the measurement. (We have mini-

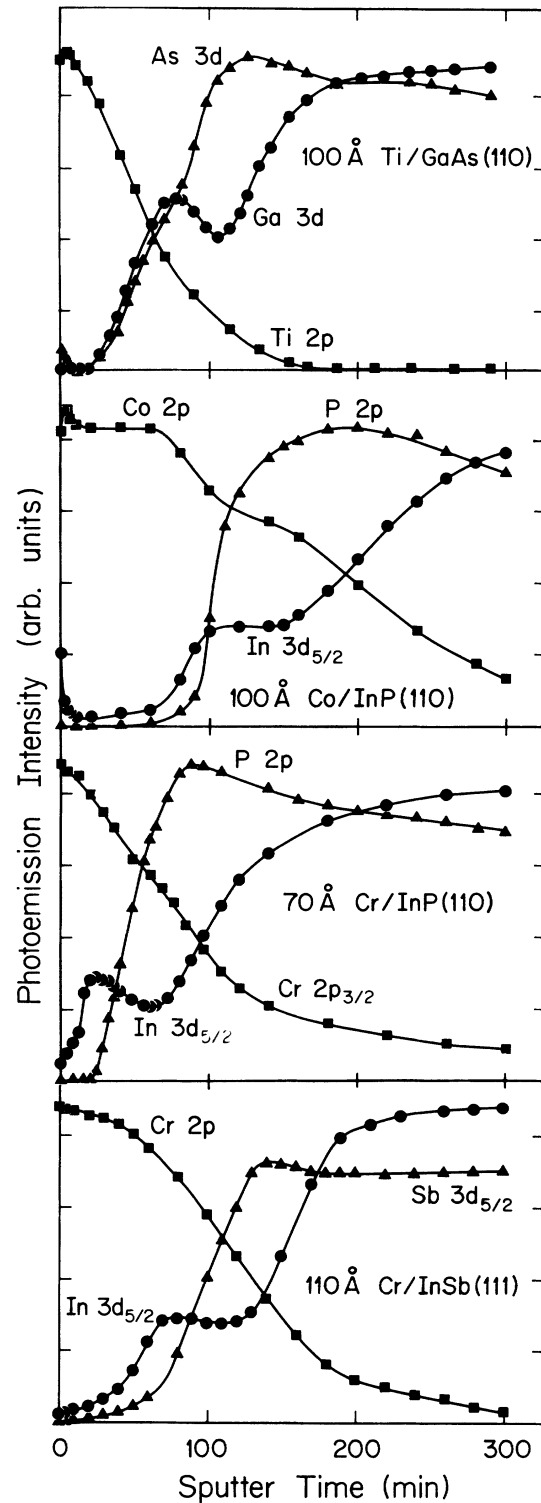


FIG. 1. Sputter depth profiles for 100- \AA Ti/GaAs(110), 100- \AA Co/InP(110), 70- \AA Cr/InP(110), and 110- \AA Cr/InSb(111). The vertical axes correspond to the integrated core intensities measured with XPS at an emission angle of 60° with respect to the surface normal. The As and Ga intensities are corrected by their cross section ratios as measured for the clean surface. The valleylike structures in the cation concentration curves are a result of cation expulsion from the region where metal-anion compound formation occurs.

mized this broadening by measuring photocurrents at 30° take-off angle, reducing the effective probe depth by a factor of 0.5). Third, extended sputtering can increase surface roughness and alter the erosion rates. Finally, since photoelectrons from core levels of different species have different kinetic energies, the probed region varies for each species. These effects make quantitative analysis impossible and the intensity profiles should not be seen as concentration profiles. On the other hand, they provide direct and unambiguous qualitative information about the species distributions normal to the surfaces and are particularly useful for interfaces with reactive metals where systematic behaviors are sought.

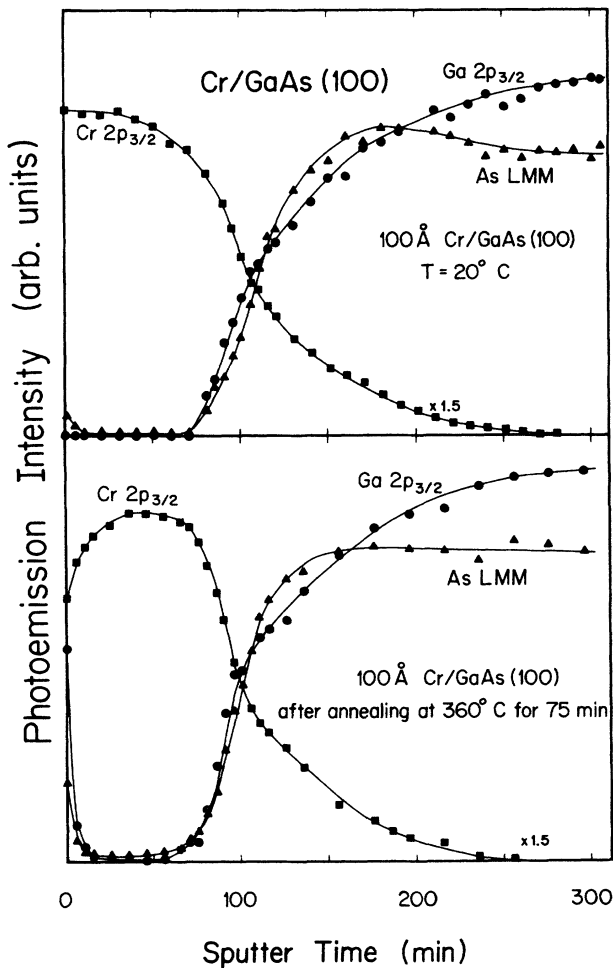


FIG. 2. Sputter profiles of 100-Å Cr/GaAs(100) interface at room temperature and after annealing at 360°C for 75 min. The As LMM Auger peak was used because of the overlap of the Cr 3p and As 3d emission. The Ga and As intensities are normalized to their cross section ratios. At room temperature, the anion and cation concentrations decay smoothly from the substrate into the overlayer. After annealing, a substantial number of both As and Ga atoms are segregated to the surface. This indicates that a large fraction of the anions and cations released during interface formation at room temperature are weakly bonded in the Cr matrix and are expelled when a more perfect Cr layer can grow.

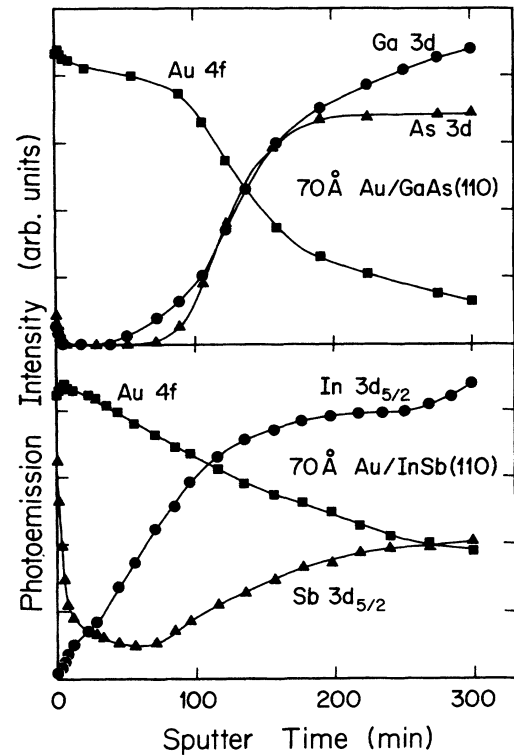


FIG. 3. Species concentration curves across 70-Å Au/GaAs(110) and 70-Å Au/InSb(110) interfaces analogous to those of Fig. 1. Note the large anion surface segregation with respect to the cations for Au/InSb.

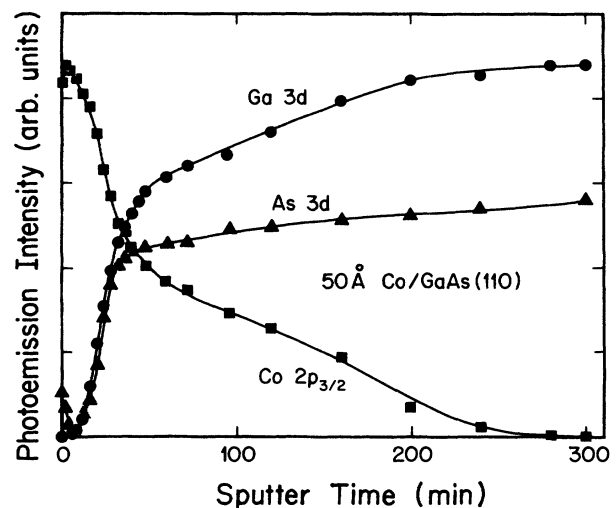


FIG. 4. Sputter profile for the epitaxial system 50-Å Co/GaAs(110). Except for a small amount of As segregation, the distribution curves are smooth and structureless. This demonstrates that epitaxy and substrate disruption are not mutually exclusive provided that the conditions for epitaxy exist and the disruption is not too severe. The Ga and As atoms are trapped as impurities in the epitaxial Co film and their concentration varies with distance from the buried interface or the surface.

RESULTS

In Figs. 1–4 we present sputter profiles for eight metal–III-V semiconductor systems. The results are grouped according to the reactivity of the deposited metal with the substrate anion, and they show similarities in their sputter profiles.

To address the problem of substrate atom distributions close to the buried interface, we emphasize the structures in the concentration profiles of Figs. 1–4. Before doing so, however, there are two important points that can be made. First, most of the profiles of Figs. 1–4 provide direct evidence of semiconductor atom segregation to the metal surface because sputtering shows a rapid loss in emission from the segregated atoms after light sputtering. This can be seen, for example, for As in Ti/GaAs (Fig. 1); In in Co/InP (Fig. 1); As in Cr/GaAs (Fig. 2); Ga, As, and Sb for Au/GaAs and InSb (Fig. 3); and for As in Co/GaAs (Fig. 4). This observation of segregation is consistent with the conclusions of Ref. 16 where results from the literature were analyzed for 28 interfaces. That paper showed that the relative cohesive energies and atomic sizes of semiconductors elements with respect to those of the metal determine substrate element surface segregation, assuming relatively weak chemical trapping. Second, the results of Figs. 1–4 show that the number of semiconductor atoms in the metal overlayer varies considerably, from a small value for P in Co/InP to a much higher value for Sb in Cr/InSb. The issue of solubility has been quantitatively considered for Au/GaAs and Co/GaAs and will not be dealt with here. (A concentration model was used in Refs. 17 and 18 to show that anion and cation solubilities in metal overlayers grown by evaporation at room temperature can be much larger than the values extrapolated from high-temperature equilibrium states.)

In Fig. 1 we show the sputter depth profiles for the highly reactive 100-Å Ti/GaAs(110), 100-Å Co/InP(110), 70-Å Cr/InP(110), and 110-Å Cr/InSb(111) systems. These concentration curves have a very interesting common feature, namely, that the anion distributions in the overlayer are smooth and almost structureless while those of the cations exhibit a distinct valleylike structure or a plateau. This valley reflects cation depletion near the buried interface and a piling up in front of the deficiency region.

For the clean, cleaved GaAs(110) surface, the ratio of the integrated As 3*d* to Ga 3*d* intensity is ~ 1.24 as excited with a photon energy of 1486.6 eV. (This value is never reached when the interface is sputtered for the reasons noted above.) The results of Fig. 1 show that the deposition of Ti followed by its removal by sputtering changes this ratio, giving a maximum value of 2.7 in the region near the buried interface and a value of only 0.95 beyond this layer. Since As 3*d* and Ga 3*d* photoelectrons have the same mean free path, these intensity variations reveal changes in the atomic concentration within the probed region (3λ or ~ 60 Å). To determine whether this valleylike structure in the Ga concentration profile is a characteristic of the interface at the initial stages of formation and is independent of further metal deposition, we under-

took measurements with different Ti overlayer thicknesses (≥ 30 Å) as well as for a reconstructed GaAs(100) surface.^{19,20} These results showed no change except for an increase in separation between the Ga peak and the vacuum surface. Analogous studies of the In concentration profiles for Cr/InP(110) and Cr/InSb(111) interfaces, as well as Ti/InP(110), showed similar valleylike structures for In, indicating that the structure is not unique to Ga.

Although the valleylike structure is common for reactive metal overlayers, it is not always as pronounced as for Ti/GaAs or Cr/InP. Indeed, the sputter profiles for 100-Å Co/InP(110) showed it to be reduced to a plateau and, further, that the ratio of In to P is smaller. For Cr/InSb(111), we find intermediate behavior and a weak minimum near the buried interface. The similarity in cation depletion, but the variability in the amount of cation accumulation, suggests that these distributions reflect a common expulsion mechanism with differences related to the amount of surface segregation and interface solubilities. These differences are then specific to the cations and metals under study.

In order to determine whether these anion and cation profiles are metastable with respect to temperature, we formed 100-Å Cr/GaAs(110) interfaces at room temperature and compared the profiles to those obtained for identical interfaces after annealing at 360°C for 75 min. The results summarized in Fig. 2 show that the Cr-GaAs interaction is relatively weak²¹ and does not produce the Ga valley structure. Instead, there is a monotonic decrease in both Ga and As intensities away from the substrate and this characteristic was important for these temperature-dependent studies. As shown, annealing at 360°C increases the Ga and As content of the surface and the near-surface region, and the Ga and As profiles at the buried interface become sharper. We conclude that substantial amounts of dissociated Ga and As atoms weakly bonded to Cr exist in the intermixed region near the buried interface as a consequence of room-temperature substrate disruption. Heating increases the diffusion of these impuritylike atoms and promotes their segregation to the surface. The result is that the Cr layer becomes more perfect and the free energy of the system is lowered.

To investigate the profiles for metal–III-V systems where metal-cation reaction is favored over metal-anion reaction (but is still very weak at room temperature), we formed the Au/GaAs(110) and Au/InSb(110) interfaces. The results shown in Fig. 3 indicate that the Ga and As concentrations decay smoothly from the substrate into the Au overlayer, that limited amounts of Ga and As are dissolved in the Au matrix, and that both species segregate to the free surface. These results for Au/GaAs confirm our earlier studies^{17,22} and are consistent with those reported by Spicer and co-workers.²³

Finally, we have investigated the 50-Å Co/GaAs interface because earlier work showed bcc Co to grow epitaxially. At the same time, those studies showed substrate disruption at low coverage followed by segregation of As to the surface and the dissolution of small amounts of Ga and As. As shown in Fig. 4, our sputtering profiles again find evidence for As surface segregation but there is no

valleylike structure in the cation profile. These results provide a baseline for comparison to systems where intermixing is greater and reaction products form.

As part of our investigations of interface formation, we

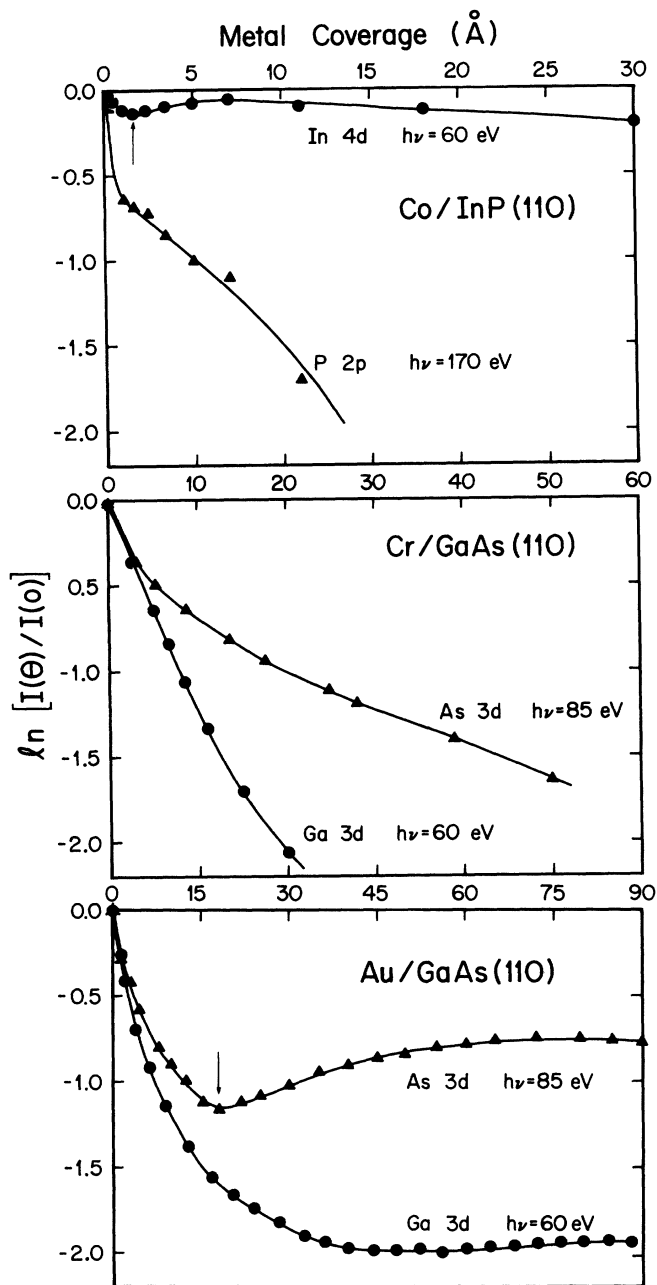


FIG. 5. Substrate element core photoemission intensity attenuation curves $\ln[I(\Theta)/I(0)]$ as a function of nominal metal coverage, Θ for Co/InP(110), Cr/GaAs(110), and Au/GaAs(110). Photon energies were chosen to give maximum surface sensitivity (probed region 10–12 Å). For Co/InP, the In 4d intensity increases because of the expulsion of In atoms from the region where Co-P compound formation occurs (from Ref. 24). For Au/GaAs, the onset of As segregation reflects the convergence of the overlayer to an elemental Au film (from Ref. 5). For Cr/GaAs, there is no strong driving force for Cr-Ga or Cr-As compound formation and the disrupted semiconductor atoms are trapped in supersaturated solution (from Ref. 21).

undertook synchrotron radiation photoemission studies for Co/InP(110), Cr/GaAs(110), and Au/GaAs(110). In Fig. 5 we show attenuation curves for the various core levels, defined as $\ln[I(\Theta)/I(0)]$, where $I(\Theta)$ is the integrated intensity of a particular core level at a coverage Θ and $I(0)$ is the emission from that core for the clean surface. Incident photon energies were chosen to give inelastic mean free paths of 4–5 Å to maximize the surface sensitivity. For Co/InP(110), the In 4d intensity decreases as the Co deposition increases until a critical coverage of 1.6 Å (see Ref. 4). It then increases steadily until the nominal Co coverage reaches 7 Å and, thereafter, attenuates very slowly. Simultaneously, the P 2p signal drops rapidly, excluding the possibility of cluster formation. These results indicate that there is a coverage at which In surface segregation is triggered and In atoms are driven to the vacuum surface. Such cation surface segregation onsets have been observed for other systems.²⁴ For Cr/GaAs(110), the Ga 3d and As 3d attenuation curves are smooth and structureless with the rate of Ga loss greatly exceeding that of As because of As surface segregation (see Ref. 21). Surprisingly, for Au/GaAs(110) there is an increase in the As intensity at a nominal Au coverage of ~18 Å (see Ref. 5). This rise in intensity reflects an increase in As concentration on the surface, analogous to that for In at the reactive Co/InP(110) interface. Since Au does not react with Ga or As to form compounds at room temperature, the physical mechanism that triggers this anion surface segregation differs somewhat from that for cation atoms in reactive systems while still being related to free-energy minimization, as will be discussed in the next section.

DISCUSSION

When metal atoms are deposited from the vapor phase onto clean III-V semiconductor surfaces, they can chemisorb reactively or they can form small clusters or patches. As a result, they change the overall energy configuration of the near-surface bonds and can weaken or break anion-cation covalent bonds. These released atoms can diffuse into the overlayer to form compounds or alloys with the metal adatoms, including solid solutions. Disruption and direct reaction continues until the reaction product becomes a self-limiting diffusion barrier. Thereafter, the metal nucleates, possibly incorporating some semiconductor atoms or forcing their segregation to its surface. Factors which control the concentration profile include the extent of substrate disruption (and thus the number of the released anions and cations), the chemical reactivities of the metal with the anions or cations, the stability of the reaction products (if there are any), and the semiconductor atom solubilities in the metal and in the reaction products.

To identify the tendencies for reaction for the interfaces under study here, we list in Table I the heats of compound formation for metals and substrate anions, as well as GaAs, InP, and InSb. These results indicate that energetically stable Ti-As, Ti-P, Co-P, and Cr-P compounds could form. No thermodynamical values are available for Cr-Sb compounds, but recent results by Bos-

TABLE I. Heats of compound formation in kJ/mol^{-1} from the *National Bureau of Standards Tables of Chemical Thermodynamical Properties* [J. Phys. Chem. Ref. Data **11** (Suppl. 2) (1982)].

GaAs	-71	InP	-88.7	InSb	-30.5
TiAs	-149.8	TiP	-282.8	TiSb	-281.2
Co ₂ As	-39.7	Co ₂ P	-188	CoSb	-42
CoAs	-40.6			CoSb ₂	-54
CoAs ₂	-61.5			CoSb ₃	-67
Co ₅ As ₂	-79.5			AuSb ₂	-10.9
Co ₃ As ₂	-81.2			AuIn	-45.2
Co ₂ As ₃	-97.5			AuIn ₂	-75.3

cherini *et al.*²⁵ suggest that Cr-Sb compounds may exist at Cr/InSb interface, and the small heat of formation of InSb (-30.5 kJ/mol) favors this. In contrast, Cr-As compounds are less favorable than GaAs itself and the Cr-As bond is expected to be weak. For the cations, there is no indication that compounds would form and alloy formation is unlikely at room temperature (Au-Ga and Au-In are the exceptions). One should be cautious, however, because these thermodynamic values are for bulk systems in equilibrium states—not for interface reactions far from equilibrium.

In the following, we will use this information, together with the results from Figs. 1–5 and the literature, to describe the physical formation of metal-III-V semiconductor interfaces.

Ti/GaAs, Co/InP, Cr/InP, and Cr/InSb

Synchrotron-radiation photoemission studies for these interface systems have shown that the metal adatoms react strongly with the anions P, As, and Sb and the cations are dissolved in the overlayer with no well-defined bonding configurations, consistent with the thermodynamic information (Ruckman *et al.*,²⁶ Ludeke and Landgren,²⁷ and Xu *et al.*^{12,19} for Ti/GaAs; Kendelwicz *et al.*²⁸ and Xu *et al.*²⁴ for Co/InP and Cr/InP; Boscherini *et al.*²⁵ for Cr/InSb). As the amount of deposited metal increases, the metal-anion nuclei increase in number and grow in size both laterally and vertically. Xu *et al.*²⁴ have shown through studies of Co/InP(110) that there is a critical metal coverage at which the Co-P nuclei reach sufficient concentration and size that the cations are expelled from the compound regions. The resulting cation surface segregation lowers the free energy of the system. Reaction and segregation continue until the intermixed region serves as an effective buffer layer to kinetically limit atomic intermixing. At that stage, the cation expulsion is completed, the concentration of cations on the surface region is high, and there is a region below the surface where there is a paucity of cations. With subsequent deposition, the expelled cations are ultimately dissolved in the metal layer at a rate determined by nonequilibrium solubilities. We propose that this mechanism of cation expulsion is quite general for many highly reactive systems and is responsible for the depletion regions in the concentration profiles of Fig. 1. The synchrotron radiation photoemission studies cited above and the present sputter profiling results give complementary information about interface evolution.

The results for Ti/GaAs shown in Fig. 1 reflect this atomic distribution for a system grown at room temperature. Heating of this interface enhances Ti-As reaction and expands the region over which compound formation occurs, resulting in the retreat of the buried interface.¹² There is also enhanced Ga expulsion from the region where Ti-As forms and there is a promotion of Ga surface segregation. Indeed, the Ga concentration close to the buried interface is only a few atomic percent after annealing at 365°C for 2.5 h and the Ga density is very high in the near-vacuum surface region. This distribution has been confirmed by both *in situ* x-ray photoemission¹² and the x-ray diffraction measurements of Wada *et al.*²⁹ Although analogous annealing studies have not been reported for the other systems shown in Fig. 1, we propose that additional compound formation at the buried interface would result in sharpening of the cation profiles and greater segregation, provided ternary phase formation is not favored.

Cr/GaAs

For the Cr/GaAs system, Weaver *et al.*²¹ and Williams *et al.*³⁰ have demonstrated that Cr does not react strongly with As to form a stable Cr-As compound at room temperature because the Cr-As bonds are relatively weak. During the early stages of formation of this system, the metal adatoms and the dissociated anions and cations intermix in the region close to the buried interface. Since Cr-As compound formation is not as compelling, there is much less cation expulsion. This is consistent with the sputter profiles for the Cr/GaAs interface grown at room temperature (top of Fig. 2). Sputter profiles taken after annealing at 360°C for 75 min show that heating promotes both Ga and As surface segregation, indicating that large amount of weakly bonded Ga and As atoms exist in the intermixed region when the interface is formed at room temperature. In this configuration, they present a high-energy, metastable state. Annealing leads to a state of lower free energy by promoting the formation of a purer form of Cr near the buried interface and throughout much of the overlayer.

Co/GaAs and Co/InP

Xu *et al.*¹⁸ and Prinz *et al.*³¹ recently investigated the growth and properties of Co evaporated on GaAs(110) and (100) surfaces. They observed that an ordered film of metallic bcc Co could be grown epitaxially, despite the

fact that there is limited substrate disruption. Xu *et al.*¹⁸ further reported that released As atoms do not form a Co-As compound and that both Ga and As appeared interstitially in the Co matrix. The present sputter profiles summarized in Fig. 4 reveal a smooth distribution of Ga and As in the overlayer and support the conclusions of the earlier work. The presence of segregated As at the surface is a consequence of the unfavorable bonding of Co-As and the low solubility of As.

Comparison of the results for Co/GaAs in Fig. 4 to those for Co/InP in Fig. 1 emphasizes the importance of interface reaction in determining the ultimate concentration profiles in the overlayer. For both interfaces, there is good lattice matching with bcc Co ($\sim 0.18\%$ for GaAs and 3.9% for InP). However, the heats of formation for Co-P compounds favor a high degree of chemical reactivity while those for Co-As are much weaker. As a result, Co-P nuclei form readily and reaction expands both laterally and vertically with increasing Co coverage. For Co/GaAs, the disruption may be quite inhomogeneous across the surface in such a way that domains of epitaxial Co can grow directly on GaAs.

Au/GaAs and Au/InSb

A large number of Au/GaAs interface studies have been reported, and those by Spicer and co-workers,²³ Xu *et al.*¹⁷, Grioni *et al.*,⁵ and Anderson *et al.*³² are particularly relevant to the present paper. It is generally agreed that Au adatoms induce disruption of the substrate but do not form Au islands or compounds at room temperature. Instead, there are high concentrations of Ga and As atoms in this intermixed region and these semiconductor atoms are essentially in a metastable, supersaturated solution. Substrate disruption is completely by coverages of 10–15 Å. The synchrotron-radiation attenuation curves for Ga and As shown in Fig. 5 reveal a very surprising increase in the As intensity at Au coverages of ~ 18 Å. This onset of *anion* surface segregation is of interest here because the interface reactions are different from those discussed above. In particular, the onset of As segregation toward the surface cannot be due to expulsion from a reacting Au-Ga alloy region as was the case when In was expelled from Co-P regions. Instead, we suggest that it is the formation of increasingly pure Au aggregates that expels the As to the surface. The observation is analogous to that found in Fig. 2 where annealing was needed to expel Ga and As from supersaturated solution in Cr. These expelled As atoms float on the Au film because of their low solubility in *pure* Au of a critical dimension. This is reflected in the attenuation curves, the magnitude of the segregated As, and the absence of a valley structure in the As distribution profile of Fig. 3. Since Au—Ga bonding is more

favorable, there is a greater chance of nuclei of Au-Ga or a higher solubility in Au. Hence, there is weaker expulsion and a much lower concentration of segregated Ga. Analogous behavior can be seen for Au/InSb(110) although there is greater substrate disruption and an even higher Sb concentration on the Au surface.

Support for this anion segregation onset model comes from a photoemission study of Ruckman *et al.*³³ of the binary Au/Ge system where a similar rise in the attenuation curves for Ge was observed at a nominal Au coverage of 15–20 Å. In this case it is obvious that Ge expulsion toward the free surface cannot be caused by the formation of a Au-Ge phase. Instead, those results can be interpreted in terms of the energy lowering of the interior of the film as purer Au forms and Ge is driven to the surface. It appears that a Au film of high purity decorated by a skin with a high concentration of semiconductor atoms is thermodynamically favored over the supersaturated solution or any compound at room temperature. This is no longer the case, of course, when Au-Ga compound formation is made possible by thermal processing.³⁴

In this paper we have sought a unified mechanism that describes the observations of a wide variety of experiments, including the present sputter profiles and synchrotron radiation photoemission measurements. For transition-metal-III-V compound-semiconductor systems, the metal-anion chemical reactions and the properties of those reaction products are very important in understanding the atomic distribution. We have demonstrated that cation atoms can be expelled from the metal-anion compound region as it evolves from a collection of small nuclei into a phase with appreciable dimension. An analogous behavior is observed for noble-metal-III-V compound-semiconductor systems but it is the evolution of Au nuclei that is critical since they are the lowest-energy configuration. We have also shown that the onset of surface segregation, the extent of the cation-deficient region, and the amount of the expelled cation atoms depend on many other factors, including the amount of compound formation, the number of dissociated cations, and the solubilities of cation atoms in the compound regions.

ACKNOWLEDGMENTS

We thank I. M. Vitomirov, C. M. Aldao, and Y. Shapira for many stimulating discussions. This work was supported by the Office of Naval Research under Contracts No. N00014-87-K-0029 and No. N00014-86-K-0427. The soft-x-ray photoemission experiments were done at the NSF-supported Wisconsin Synchrotron Radiation Center.

*Permanent address: Institute of Physics, Chinese Academy of Sciences, Beijing, People's Republic of China.

¹A great many important contributions have come from the application of the tools of surface science for interface research,

including those listed in Refs. 2–10. Others would, of course, include scanning tunneling microscopy, LEED, medium-energy ion scattering, and Rutherford backscattering. References 2–10 emphasize photoemission of the sort that will be

- discussed here.
- ²W. E. Spicer, P. W. Chye, P. R. Skeath, C. Y. Su, and I. Lindau, *J. Vac. Sci. Technol.* **16**, 1422 (1979); W. E. Spicer, I. Lindau, P. Skeath, C. Y. Su, and P. Chye, *Phys. Rev. Lett.* **44**, 420 (1980); W. E. Spicer, I. Lindau, P. Skeath, and C. Y. Su, *J. Vac. Sci. Technol.* **17**, 1019 (1980).
- ³L. J. Brillson, *Surf. Sci. Rep.* **2**, 123 (1982), and references therein; L. J. Brillson, C. F. Brucker, N. G. Stoffel, A. D. Katnani, and G. Margaritondo, *Phys. Rev. Lett.* **46**, 838 (1981).
- ⁴J. R. Waldrop, S. P. Kowalczyk, and R. W. Grant, *J. Vac. Sci. Technol.* **21**, 607 (1982).
- ⁵M. Grioni, J. J. Joyce, and J. H. Weaver, *J. Vac. Sci. Technol. A* **4**, 965 (1986); J. J. Joyce, M. Grioni, M. del Giudice, M. W. Ruckman, F. Boscherini, and J. H. Weaver, *J. Vac. Sci. Technol. A* **5**, 2019 (1987).
- ⁶T. Kendelewicz, W. G. Petro, I. Lindau, and W. E. Spicer, *J. Vac. Sci. Technol. B* **2**, 453 (1984).
- ⁷A. Fujimori, M. Grioni, and J. H. Weaver, *Phys. Rev. B* **33**, 726 (1986).
- ⁸G. Hughes, R. Ludeke, F. Schaffler, and D. Rieger, *J. Vac. Sci. Technol. B* **4**, 924 (1986).
- ⁹R. A. Butera, M. del Giudice, and J. H. Weaver, *Phys. Rev. B* **33**, 5435 (1986).
- ¹⁰K. L. I. Kobayashi, N. Watanabe, T. Narasawa, and H. Nakashima, *J. Appl. Phys.* **58**, 3758 (1985); N. Watanabe, K. L. I. Kobayashi, T. Narasawa, and H. Nakashima, *J. Appl. Phys.* **58**, 3766 (1985).
- ¹¹S. A. Chambers, D. M. Hill, F. Xu, and J. H. Weaver, *Phys. Rev. B* **35**, 634 (1987).
- ¹²F. Xu, Z. Lin, D. M. Hill, and J. H. Weaver, *Phys. Rev. B* **35**, 9353 (1987); **36**, 6624 (1987).
- ¹³M. del Giudice, J. J. Joyce, M. W. Ruckman, and J. H. Weaver, *Phys. Rev. B* **35**, 6213 (1987).
- ¹⁴I. L. Singer, J. S. Murday, and L. K. Cooper, *Surf. Sci.* **108**, 7 (1981).
- ¹⁵Y.-X. Wang and P. H. Holloway, *J. Vac. Sci. Technol. B* **2**, 613 (1984).
- ¹⁶Z. Lin, F. Xu, and J. H. Weaver, *Phys. Rev. B* **36**, 5777 (1987).
- ¹⁷F. Xu, Y. Shapira, D. M. Hill, and J. H. Weaver, *Phys. Rev. B* **35**, 7417 (1987).
- ¹⁸F. Xu, J. J. Joyce, M. W. Ruckman, H.-W. Chen, F. Boscherini, D. M. Hill, S. A. Chambers, and J. H. Weaver, *Phys. Rev. B* **35**, 2375 (1987).
- ¹⁹F. Xu, D. M. Hill, Z. Lin, S. G. Anderson, Y. Shapira, and J. H. Weaver, *Phys. Rev. B* **37**, 10295 (1988).
- ²⁰F. Xu, D. M. Hill, Z. Lin, and J. H. Weaver (unpublished).
- ²¹J. H. Weaver, M. Grioni, and J. J. Joyce, *Phys. Rev. B* **31**, 5348 (1985).
- ²²Y. Shapira, F. Xu, D. M. Hill, and J. H. Weaver, *Appl. Phys. Lett.* **51**, 118 (1987); Y. Shapira, F. Boscherini, C. Capasso, F. Xu, D. M. Hill, and J. H. Weaver, *Phys. Rev. B* **36**, 7656 (1987).
- ²³P. W. Chye, I. Lindau, P. Pianetta, C. M. Garner, C. Y. Su, and W. E. Spicer, *Phys. Rev. B* **18**, 5545 (1978); W. G. Petro, T. Kendelewicz, I. Lindau, and W. E. Spicer, *ibid.* **34**, 7089 (1986); D. Coulman, N. Newman, G. A. Reid, Z. L. Weber, E. R. Weber, and W. E. Spicer, *J. Vac. Sci. Technol. A* **5**, 1521 (1987).
- ²⁴F. Xu, C. M. Aldao, I. M. Vitomirov, Z. Lin, and J. H. Weaver, *Phys. Rev. B* **36**, 3495 (1987); C. M. Aldao, I. M. Vitomirov, F. Xu, and J. H. Weaver, *ibid.* **37**, 6019 (1988).
- ²⁵F. Boscherini, Y. Shapira, C. Capasso, C. M. Aldao, and J. H. Weaver, *J. Vac. Sci. Technol. B* **5**, 1003 (1987).
- ²⁶M. W. Ruckman, M. del Giudice, J. J. Joyce, and J. H. Weaver, *Phys. Rev. B* **33**, 2191 (1986).
- ²⁷R. Ludeke and G. Landgren, *Phys. Rev. B* **33**, 5526 (1986).
- ²⁸T. Kendelewicz, R. S. List, M. D. Williams, K. A. Bertness, I. Lindau, and W. E. Spicer, *Phys. Rev. B* **34**, 558 (1986).
- ²⁹O. Wada, S. Yanagisawa, and H. Takanashi, *Appl. Phys. Lett.* **29**, 263 (1976).
- ³⁰M. D. Williams, T. Kendelewicz, R. S. List, N. Newman, C. E. McCants, I. Lindau, and W. E. Spicer, *J. Vac. Sci. Technol. B* **3**, 1202 (1985).
- ³¹G. A. Prinz, *Phys. Rev. Lett.* **54**, 1051 (1985).
- ³²T. G. Andersson, J. Kanski, G. Le Lay, and S. P. Svensson, *Surf. Sci.* **168**, 301 (1986).
- ³³M. W. Ruckman, J. J. Joyce, F. Boscherini, and J. H. Weaver, *Phys. Rev. B* **34**, 5118 (1986).
- ³⁴T. Yoshiie and C. L. Bauer, *J. Vac. Sci. Technol. A* **1**, 554 (1983); T. Yoshiie, C. L. Bauer, and A. G. Milnes, *Thin Solid Films* **111**, 149 (1984); J. R. Lince, C. T. Tsai, and R. S. Williams, *J. Mater. Res.* **1**, 537 (1986); E. Beam and D. D. L. Chung, *Mater. Res. Soc. Symp. Proc.* **37**, 595 (1985).